

Temperature Dependence of Thermodiffusion in Aqueous Suspensions of Charged Nanoparticles

Shawn A. Putnam,* David G. Cahill, and Gerard C. L. Wong

Department of Materials Science and Engineering and Center of Advanced Materials for the Purification of Water with Systems, University of Illinois, Urbana, Illinois 61801

Received February 19, 2007. In Final Form: June 11, 2007

Measurements of particle flows driven by temperature gradients are conducted as a function of temperature on aqueous suspensions of polystyrene nanoparticles and proteins of T4 lysozyme and mutant variants of T4 lysozyme. The thermodiffusion coefficients are measured using a microfluidic beam deflection technique on suspensions with particle concentrations on the order of 1 vol %. At $T \lesssim 20$ °C, all of the nanoparticles studied migrate to the hot regions of the fluid; i.e., the thermodiffusion coefficient is negative. At higher temperature, $T \gtrsim 50$ °C, the thermodiffusion coefficient is positive with a value consistent with the predictions of a theoretical model originally proposed by Derjaguin that is based on the enthalpy changes due to polarization of water molecules in the double layer.

1. Introduction

Thermodiffusion, the phenomenon of mass transport in a temperature gradient, was observed experimentally by Ludwig in 1856 and then 20 years later in salt solutions by Soret.¹ Thermodiffusion, also known as the Soret effect, thermal diffusion, and thermophoresis, is typically characterized by either the Soret coefficient S_T or the thermodiffusion coefficient D_T . At small particle concentrations c_p , the particle flux of a colloidal suspension in a temperature gradient ∇T is $\mathbf{J} = -c_p D_T \nabla T - D_c \nabla c_p$, where D_c is the mass diffusion coefficient, and $S_T = D_T/D_c$.

In recent years, considerable experimental and theoretical effort has focused on the thermodiffusion of particles in liquids.² A theoretical understanding of the motion of particles in temperature gradients is attractive, because thermodiffusion is predicted to provide insight into the thermodynamics of the interface between the nanoparticle and the surrounding solvent.³

Experimental investigations on the thermodiffusion of particles in liquids have examined a wide variety of different solvent–particle systems: e.g., colloidal particles, electrolytes, micelles, polymers, proteins, and DNA.² Several theoretical descriptions have been proposed that incorporate a variety of fundamental mechanisms as explanations for the thermally driven particle flows in liquids: interfacial tension gradients,⁴ nonuniform electrolyte and electrostatic distributions,⁵ thermal–acoustic perturbations,⁶ radiation pressures,⁷ and nonuniform London–van der Waals interactions.⁸ Yet, despite the long history of theoretical effort on the subject, a generally accepted theory for thermodiffusion has not been established.^{9–11}

To help address this situation, we have conducted thermodiffusion experiments as a function of temperature on aqueous

suspensions of (1) charged polystyrene (PS) nanoparticles of varying particle diameters and (2) lysozyme proteins of different formal charge. We also limit these studies to low ionic strength, $I \lesssim 1.3$ mM, to minimize contributions due to the coupling between the thermodiffusion of ions in the electrolyte and the thermodiffusion of the nanoparticles.¹²

We observe essentially the same behavior for all nanoparticle suspensions studied: that is, the particles move toward the hot regions of the fluid at $T \lesssim 20$ °C, and at higher temperatures, typically $T \gtrsim 30$ °C, the particles move toward the cold regions of the fluid. This same qualitative temperature dependence has recently been observed by others.^{9,10,13–15} We show, however, that in the high-temperature limit the thermodiffusion coefficient is quantitatively consistent with a theoretical model that is based on the changes in enthalpy density of the solvent molecules in the double layer. This model was originally proposed by Derjaguin¹⁶ to describe fluid flow in porous media and then later adapted by Anderson³ to describe particle flow. If the change in enthalpy density $h(y)$ is dominated by the polarization of water molecules by the electric fields in the double layer, then $h(y) = 1/2(\epsilon + T\partial\epsilon/\partial T)E^2(y)$, where ϵ is the dielectric constant of water and $E(y)$ is the electric field at a distance y from the surface of the charged particle.

In our experiments, we use a microfluidic beam-deflection technique to observe the amplitude and phase of particle concentration gradients produced by a periodic temperature gradient.¹⁷ Typically, our technique is limited to particle concentrations $c_p > 0.3$ vol % to obtain sufficient signal-to-noise to accurately determine the Soret coefficient S_T . In this work, we employ particle concentrations c_p on the order of 1 vol %; yet, during the course of our work, we have varied c_p in our experiments by a factor of ~ 3 for lysozyme and a factor of ~ 5 for polystyrene and have not observed any significant changes in S_T over this limited concentration range. This result is consistent with our previous studies.¹² Nevertheless, we cannot rule out

* sputnam@uiuc.edu.

- (1) Platten, J. K.; Costesèque, P. *Eur. Phys. J. E* **2004**, *15*, 235–239.
- (2) Brenner, H. *Phys. Rev. E* **2006**, *74*, 036306.
- (3) Anderson, J. L. *Ann. Rev. Fluid. Mech.* **1989**, *21*, 61–99.
- (4) Ruckenstein, E. *J. Colloid Interface Sci.* **1981**, *83*, 77–81.
- (5) Morozov, K. I. *J. Exp. Theor. Phys.* **1999**, *88*, 944.
- (6) Andreev, A. F. *Sov. Phys. JETP* **1988**, *67*, 117–120.
- (7) Gaeta, F. S. *Phys. Rev.* **1969**, *182*, 289.
- (8) Semenov, S.; Schimpf, M. *Phys. Rev. E* **2004**, *69*, 011201.
- (9) Duhr, S.; Braun, D. *Proc. Natl. Acad. Sci. U.S.A.* **2006**, *103*, 19678.
- (10) Ning, H.; Buitenhuis, J.; Dhont, J. K. G.; Wiegand, S. *J. Chem. Phys.* **2006**, *125*, 204911.
- (11) Parola, A.; Piazza, R. *J. Phys.: Condens. Matter* **2005**, *17*, S3639.

- (12) Putnam, S. A.; Cahill, D. G. *Langmuir* **2005**, *21*, 5317–5323.
- (13) Ning, H.; Kita, R.; Krieger, H.; Luettmmer-Strathmann, J.; Wiegand, S. *J. Phys. Chem. B* **2006**, *110*, 10746.
- (14) Iacopini, S.; Piazza, R. *Europhys. Lett.* **2003**, *63*, 247–253.
- (15) Iacopini, S.; Rusconi, R.; Piazza, R. *Eur. Phys. J. E* **2006**, *19*, 59.
- (16) Derjaguin, B. V.; Churaev, N. V.; Muller, V. M. In *Surface Forces*; Kitchener, J. A., Ed.; Consultants Bureau: New York, 1987; Chapter 11, pp 390–409.
- (17) Putnam, S. A.; Cahill, D. G. *Rev. Sci. Instrum.* **2004**, *75*, 2368.

that particle–particle interactions^{18,19} are playing an important role in our experiments. Studies by Wiegand and co-workers¹⁰ reached the conclusion that particle–particle interactions were unimportant for $c_p \lesssim 10$ vol %. The recent study by Duhr et al.,⁹ on the other hand, accessed extremely small PS concentrations $c_p \lesssim 10^{-6}$ vol % using single-particle tracking and noted that these extremely small values of c_p are needed to obtain the true single-particle behavior. In what follows, we compare our experimental results to theories that have been developed for the thermodiffusion of isolated particles but must keep in mind that we are uncertain about the importance of particle–particle interactions in our data.

2. Experimental Details

Materials and Preparation of Nanoparticle Suspensions. The nanoparticle suspensions used in this study consisted of carboxyl-functionalized polystyrene (PS) spheres, proteins of T4 bacteriophage lysozyme (T4L), and mutant variants of T4L suspended in water at low ionic strength, $I \approx 1.3$ mM, and small particle concentrations $c_p \lesssim 2$ vol %.

The ionic strengths, I , were derived from measurements of the pH and ionic conductivity g , assuming NaCl was the electrolyte.¹² The particle concentrations c_p of each suspension were determined by measuring the index of refraction of the suspension with an Abbe refractometer and then calculating c_p using effective medium theory;²⁰ e.g., eq 6.3 in ref 20. Yet, in the limit of small volume fraction c_p and small contrast in properties between the phases, all effective medium theories are equivalent and reduce to a volume-weighted average $n \approx (1 - c_p)n_{\text{H}_2\text{O}} + c_p n_p$, where $n_{\text{H}_2\text{O}} = 1.3326$ is the index of refraction of water and n_p is the index of refraction of PS²¹ ($n_p = 1.59$) or lysozyme²² ($n_p = 1.53$) at 590 nm and 25 °C. Our index measurements with the refractometer were accurate within ± 0.0001 ; therefore, particle concentrations were accurate to 0.1 vol %.

Carboxyl-functionalized PS nanoparticles in water were purchased from Interfacial Dynamics Corporation (IDC).²³ Five different PS suspensions with different particle diameters and surface charge densities σ were studied. The particle diameters and surface charge densities for each suspension were characterized by the manufacturer by transmission electron microscopy (TEM) and conductometric titration, respectively. PS suspensions were prepared by diluting as-received suspensions with deionized (DI) water to $c_p \lesssim 2$ vol %. The pH was not controlled, because previous tests with buffered PS suspensions at low ionic strength showed that even small amounts of buffer (1–3 mM) would significantly affect the value of S_T . The properties of each PS suspension are provided in Table 1.

Protein suspensions of T4 bacteriophage lysozyme (T4L) and mutant variants of T4L in water were prepared by following the synthesis and purification procedures described in ref 24. Mutant variants of T4L were constructed by site-directed mutagenesis,²⁴ changing the total electrostatic charge of the wild-type (WT) T4L protein from +9 to +3. Three mutant forms of T4L were studied, consisting of either a single mutation (+7), double mutation (+5), or triple mutation (+3), where +9 is the formal or net charge of WT T4L at 5.3 pH. The shorthand notations for the single, double, and triple mutants were 154, 16/119, and 16/135/147, respectively; see ref 24. The samples were not repeatedly crystallized. After separating the proteins out on a column, they were dialyzed against water for several days before aliquoting and freezing. No additional salts or

Table 1. Suspension Properties for Carboxyl-Functionalized PS Nanoparticles in Water (pH $\approx 6.5 \pm 0.5$)^a

diameter (nm)	σ (mC/cm ²)	c_p (vol %)	I (mM)	μ_E (10 ⁴ cm ² /s·V)	ζ (mV)
26 ± 6	−0.5	2.1	1.3	−5.2 ± 0.9	−96 ± 17
34 ± 8	−0.4	1.6	0.7	−4.9 ± 0.3	−90 ± 5
67 ± 9	−0.6	1.4	0.6	−4.9 ± 0.2	−85 ± 4
90 ± 11	−7.2	1.4	1.3	−4.5 ± 0.2	−75 ± 4
92 ± 15	−0.1	1.5	0.5	−5.0 ± 0.7	−85 ± 11

^a The particle diameters and surface charge densities σ are the values reported by IDC. The surface charge densities σ are for particles in their fully charged state. The particle concentrations c_p , ionic strengths I , pH, and electrophoretic mobilities μ_E are our measurements. The ζ -potentials are estimates based on μ_E measured for these nanoparticles at $c_p = 0.3$ vol %.

Table 2. Suspension Properties for Proteins of T4L and Mutant Variants of T4L in Water (pH $\approx 5.6 \pm 0.4$)^a

protein suspension	formal charge	c_p (mg/mL)	g ($\mu\text{S}/\text{cm}$)	I (mM)	ζ (mV)
WT T4L	+9	22.0	510	4.0	67
single-mutant	+7	17.6	224	1.8	57
double-mutant	+5	10.5	119	1.0	43
triple-mutant	+3	16.8	100	0.8	26

^a We approximate the hydrodynamic radius for all proteins as $R_h \approx 1.8$ nm. The ζ -potentials are our estimates taken from eq 2, where Z_{eff} is approximated as the formal charge of the protein at 5.3 pH.

buffering chemicals were used to control the pH or enhance the stability of the suspensions. The pH measured before and after thermodiffusion experiments increased by, at most, 0.3 pH units. Therefore, the changes in protein charge during experimentation were small; see, for example, the charge titration data for lysozyme^{25,26} and mutant variants of lysozyme.²⁷ Table 2 provides the solution conditions for each protein suspension.

Electrophoresis for ζ -Potential Estimates. A commercial Malvern 3000HS Zetasizer was used to measure the electrophoretic mobilities μ_E of our charged PS nanoparticles in water. Electrophoresis experiments were performed with modulated electric fields of ~ 24 V/cm at 2 kHz. Experiments were conducted with 26, 34, 67, 90, and 92 nm carboxyl spheres diluted with water to particle concentrations $c_p \lesssim 0.3$ vol %.

Our measurements of μ_E for these PS suspensions in water are listed in Table 1. Also provided in Table 1 are our estimates of the ζ -potentials for these nanoparticles based on standard theory for the electrophoresis of spherical particles;²⁸ that is, ζ -potentials are calculated from

$$\zeta = \frac{3\mu_e\eta}{2\epsilon} f_1(\kappa R_h)^{-1} \quad (1)$$

where $\epsilon = \epsilon_r\epsilon_0$ is the dielectric constant of water, η is the viscosity of water, κ^{-1} is the Debye screening length, R_h is the hydrodynamic radius of the particle, and $f_1(\kappa R_h)$ is Henry's function that interpolates between the two regimes $\kappa R_h \ll 1$ and $\kappa R_h \gg 1$. For example, if $\kappa R_h \gg 1$, then $f_1(\kappa R_h) = 1$; and for $\kappa R_h \ll 1$, $f_1(\kappa R_h) = 3/2$.

The electrophoretic mobilities of the protein suspensions were not measured due to limited volume of the samples. Instead, we estimate the ζ -potentials for these suspensions on the basis of the Debye–Hückel model for uniformly charged spheres;²⁸ i.e.

$$\zeta = \frac{eZ_{\text{eff}}}{4\pi\epsilon R_h(1 + \kappa R_h)} \quad (2)$$

(25) Imoto, T. *Biophys. J.* **1983**, *44*, 293.

(26) Tanford, C.; Roxy, R. *Biochemistry* **1972**, *11*, 2192.

(27) Luther, J. R.; Glatz, C. E. *Biotechnol. Bioeng.* **1994**, *44*, 147.

(28) Hunter, R. J. *Foundations of Colloid Science*; Oxford University Press: New York, 2002; pp 374–433.

(18) Dhont, J. K. G. *J. Chem. Phys.* **2004**, *120*, 1632.

(19) Dhont, J. K. G. *J. Chem. Phys.* **2004**, *120*, 1642.

(20) Landauer, R. *Electrical transport and optical properties of inhomogeneous materials*; American Institute of Physics: New York, 1978; pp 15–17.

(21) Ma, X.; Lu, J. Q.; Brock, R. S.; Jacobs, K. M.; Yang, P.; Hu, X.-H. *Phys. Med. Biol.* **2003**, *48*, 4165–4172.

(22) Fredericks, W. J.; Hammonds, M. C.; Howard, S. B.; Rosenberger, F. J. *Cryst. Growth* **1994**, *141*, 183–192.

(23) Interfacial Dynamics Corporation (Portland, Oregon U.S.A.) www.id-clatex.com.

(24) Dao-pin, S.; Söderlind, E.; Baase, W. A.; Wozniak, J. A.; Sauer, U.; Matthews, B. W. *J. Mol. Biol.* **1991**, *221*, 873–887.

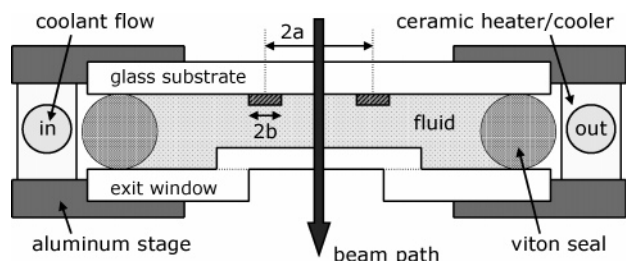


Figure 1. Schematic cross section of the temperature-controlled sample cell for measurements of thermodiffusion in liquids—not to scale. The dark, cross-hatched regions are the parallel thin-film Au line-heaters, ~ 250 nm thick, that are alternately heated at an angular frequency ω with a high-frequency square-wave current ($f_{sw} = 6.1$ kHz); e.g., the high-frequency square-wave current passes through one line-heater for the first half-cycle of ω and then through the other line-heater for the next half-cycle of ω . The line-heaters are separated by $2a = 25 \mu\text{m}$ and have a width of $2b = 5 \mu\text{m}$. The chamber height in the sampling region is $\sim 300 \mu\text{m}$.

where Z_{eff} is the effective charge of the protein at the plane-of-shear. This simple Debye-Hückel model has shown to be accurate for estimating ζ and μ_E of egg-white lysozyme and other small proteins with modified net charges.^{29,30}

Measurement Technique and Apparatus. To measure the thermodiffusion of nanoparticle suspensions, we use an optical technique based on the deflection of a laser beam passing through the fluid suspension in an applied temperature gradient. A thorough description of our apparatus and analysis methods is provided in refs 12 and 17.

Briefly, the technique produces temperature gradients by alternately heating a pair of parallel Au thin-film lines fabricated by photolithography on a fused silica (FS) substrate. As shown in Figure 1, the laser beam first passes between the parallel Au line-heaters on the FS substrate and then through the suspension within a sealed fluid cell. At low heating frequencies, $f \lesssim D_c/(\pi a^2)$, temperature gradients induce concentration gradients in the suspension due to the thermally driven transport of the particles; $2a$ is the distance between the parallel line-heaters, and $1/f$ corresponds to the time required for a particle to diffuse half the distance between the Au line-heaters. The concentration gradients created by the thermodiffusion of the particles result in an index of refraction gradient and, thus, a deflection of laser beam exiting the fluid cell. These beam deflections are measured with a position-sensitive detector and lock-in amplifier.

Our previous thermodiffusion studies using this apparatus were conducted at room temperature.^{12,17} In this work, we control the temperature of the fluid cell within the range $5^\circ\text{C} \lesssim T \lesssim 90^\circ\text{C}$ by placing a ceramic heater/cooler between the top and bottom aluminum plates of the sample stage; see Figure 1. The ceramic heater/cooler consists of a 0.13 in. o.d. copper tube wrapped with insulated 36 gauge CuNi resistance wire. The resistance wire (heater) and copper tubing (cooler) are encapsulated within a high-thermal-conductivity ceramic. The sample stage can be cooled to $T \approx -10^\circ\text{C}$ by pumping refrigerated ethanol through the copper tubing and heated to $T \approx 100^\circ\text{C}$ by running electric current through the CuNi resistance wire. We use ethanol as the coolant because of its low viscosity and freezing point. A temperature controller regulates the temperature of the fluid cell to $\pm 0.5^\circ\text{C}$. To avoid condensation on the optics and electronic contacts at temperatures below the dew point, the optical bench setup is enclosed within a plexiglass box that is purged with dry N_2 .

The temperature of the fluid is determined by measuring the resistance $\Omega(T)$ of the Au line-heaters, where $\Omega(T)$ is known from independent experiments. The temperature of the fluid can also be verified by comparing the magnitude of the measured thermo-optic

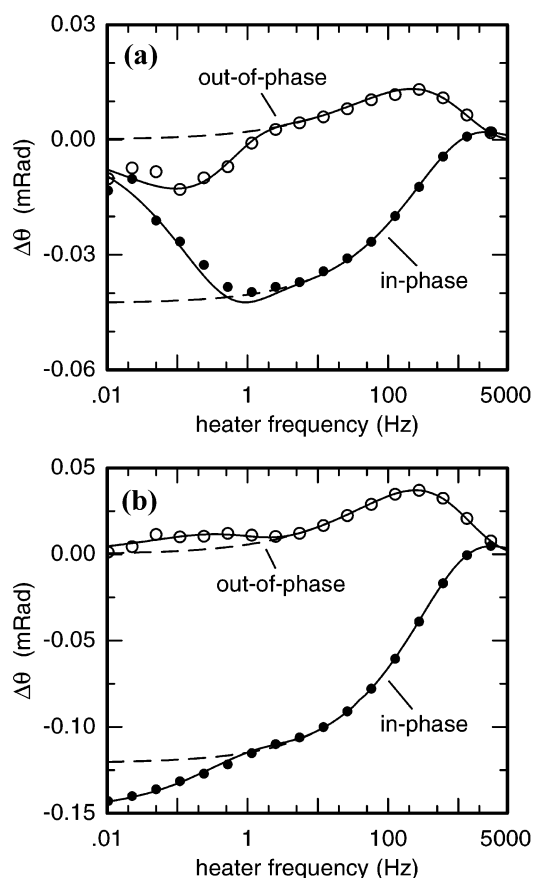


Figure 2. Comparison between experimental data (symbols) and theoretical calculations (dashed and solid lines) for the deflection of the laser beam through a protein suspension of triple-mutant T4L ($c_p \approx 16.8$ mg/mL). The solid lines correspond to single parameter fits used to determine D_T , and the dashed lines are the analytical solutions for pure water. The amplitude of the temperature oscillations are $\Delta T_{\text{osc}} \approx 1.5$ K. (a) Raw data acquired at $T \approx 10^\circ\text{C}$ for triple-mutant T4L ($D_T = -0.12 \pm 0.02 \times 10^{-7} \text{cm}^2 \text{s}^{-1} \text{K}^{-1}$, $S_T = -0.0135 \text{K}^{-1}$, $D_c = 8.6 \times 10^{-7} \text{cm}^2 \text{s}^{-1}$). (b) Raw data acquired at $T \approx 33^\circ\text{C}$ for triple-mutant T4L ($D_T = 0.12 \pm 0.04 \times 10^{-7} \text{cm}^2 \text{s}^{-1} \text{K}^{-1}$, $S_T = 0.0075 \text{K}^{-1}$, $D_c = 16.1 \times 10^{-7} \text{cm}^2 \text{s}^{-1}$).

coefficient of the water (dn/dT) with literature values.³¹ These two temperature calibrations yield fluid temperatures within $\pm 0.5^\circ\text{C}$ of each other.

Raw Data. Figure 2 shows the raw beam deflection data for triple-mutant T4L in water as a function of modulation frequency with comparisons to the analytical solution of the beam deflection $\Delta\theta$ at two different temperatures ($T \approx 10^\circ\text{C}$ and $T \approx 33^\circ\text{C}$). $\Delta\theta$ has three contributions: (1) due to thermodiffusion of the proteins, (2) due to the thermal and optical properties of water, and (3) due to the thermal and optical properties of the FS heater-substrate; e.g., $\Delta\theta = \Delta\theta|_{\text{T4L}} + \Delta\theta|_{\text{H}_2\text{O}} + \Delta\theta|_{\text{FS}}$. The contributions to $\Delta\theta$ from the FS substrate are small because $(dn/dT)_{\text{FS}} \ll (dn/dT)_{\text{H}_2\text{O}}$; thus, at high modulation frequencies, $f \gtrsim 5$ Hz, the periodic beam deflections are mainly due to the thermal and optical properties of water. However, as shown in Figure 2, at low frequencies, $f \lesssim 5$ Hz, $\Delta\theta$ has a significant contribution due to thermodiffusion of the proteins. If $D_T \rightarrow 0$, then the fitted analytical solution (solid lines) approaches the analytical solution for pure water (dashed lines).

All data reported in this study are single-parameter fits of the thermodiffusion coefficient D_T . The mass diffusion coefficient D_c is calculated from the Stokes-Einstein relation, $D_c = k_B T / 6\pi\eta R_h$, the viscosity of water η is taken from ref 32, R_h is the hydrodynamic radius of the particle, and all other model parameters are taken from

(29) Gitlin, I.; Carbeck, J. D.; Whitesides, G. M. *Angew. Chem., Int. Ed.* **2006**, *45*, 3022.

(30) Carbeck, J. D.; Colton, K. J.; Anderson, J. R.; Deutch, J. M.; Whitesides, G. M. *J. Am. Chem. Soc.* **1999**, *121*, 10671.

(31) Schiebener, P.; Straub, J.; Sengers, J. M. H. L.; Gallagher, J. S. *J. Phys. Chem. Ref. Data* **1990**, *19*, 1617.

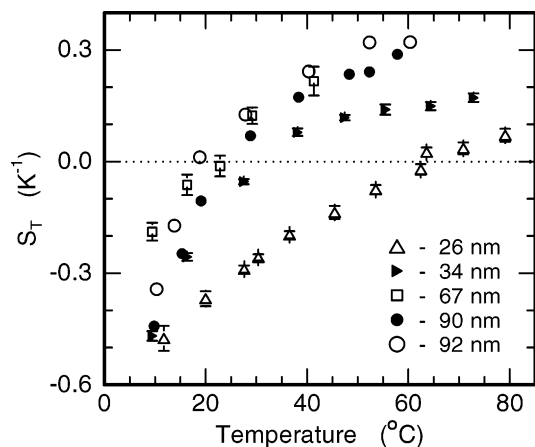


Figure 3. Soret coefficients S_T as a function of temperature for carboxyl-functionalized PS nanoparticles of different diameters in water ($\text{pH} \approx 6.5$, $\Delta T_{\text{osc}} \approx 0.6$ K). Measurement uncertainties for the 90 and 92 nm PS are comparable to that shown for the 67 nm PS.

literature or measured independently.^{33,34} D_c can, in principle, also be extracted from the frequency dependence of the data,¹² but in most cases, the uncertainties in a measurement of D_c using our methods are comparable to the uncertainties in the application of the Stokes–Einstein relation.

The onset of fluid mixing by convection limits the amplitude of the temperature oscillation ΔT_{osc} that can be used in the experiment. Typically, the effects of convection are apparent in our experiment when $\Delta T_{\text{osc}} > 3$ K; e.g., for $\Delta T_{\text{osc}} > 3$ K, we find that the magnitude of the beam deflections $\Delta\theta$ are reduced at the lowest heating frequencies. In all of the experiments reported here, $\Delta T_{\text{osc}} \leq 1$ K.

3. Results

Figure 3 shows the temperature-dependent Soret coefficients measured for the carboxyl-functionalized PS nanoparticles of different diameters purchased from IDC. All data are for suspensions diluted with water to particle concentrations $c_p \approx 2$ vol %. The suspension properties at room temperature are provided in Table 1. As shown in Figure 3, the Soret coefficients for all PS suspensions are negative at temperatures $T \lesssim 20$ °C and increase to positive values at higher temperatures.

The data for the 26 nm diameter PS spheres appear to be somewhat anomalous. We are uncertain as to why the suspension of 26 nm PS requires considerably higher temperatures than the other samples before S_T changes sign. For small-diameter latex particles, surfactant used in the polymerization is sometimes difficult to remove completely from the surface of the particles. It is possible that the thermodiffusion behavior of the 26 nm spheres is affected by this type of residual contamination.

Figure 4 shows the temperature-dependent Soret coefficients measured for the protein suspensions of T4 lysozyme (T4L) and mutant variants of T4L in water. The data are in agreement with the temperature dependence of S_T previously reported for egg-white lysozyme by Iacopini et al.¹⁴ At solution temperatures slightly greater than the highest temperature data point shown for each suspension, the proteins started to aggregate. We attribute this loss of stability to the onset of thermal denaturation; e.g.,

(32) Sengers, J. V.; Watson, J. T. R. *J. Phys. Chem. Ref. Data* **1986**, *15*, 1291.

(33) The thermal conductivity and heat capacity of water are taken from refs 32 and 51, respectively. The thermo-optic coefficient of water at 632.8 nm is calculated from the temperature dependent index of refraction data in ref 31.

(34) The heat capacity of FS is taken from ref 52. The thermal conductivity of FS is taken from ref 53, and can also be found at <http://users.mrl.uiuc.edu/cahill>. The thermo-optic coefficient of FS, $dn/dT \approx 7.5 + 0.01(T - 293.15) \times 10^{-6} \text{ K}^{-1}$, and effective beam waist of the laser focused between the metal line-heaters w_0^{cell} were determined in independent experiments with the FS substrate in air.

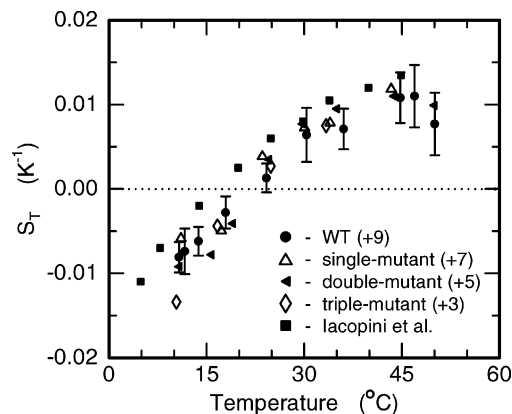


Figure 4. Soret coefficients of T4L and mutant variants of T4L in water as a function of temperature ($\text{pH} \approx 5.6$, $R_h \approx 1.8$ nm, $\Delta T_{\text{osc}} \approx 1.5$ K). Measurement errors for all proteins are comparable to that shown for WT T4L.

the midpoint temperatures for thermal unfolding at $\text{pH} \sim 5.3$ are $T_m \approx 66.7$, 64.1, 67.6, and 62.7 °C for the WT, single-mutant, double-mutant, and triple-mutant proteins, respectively.²⁴

Single and multiple mutations of T4L do not significantly change the tertiary structure of the protein.^{24,35} In this work, as shown in Figure 4, we also find that changing the formal charge of WT T4L from +9 to +3 does not significantly change the magnitude or temperature dependence of S_T . As we discuss in detail below, many of the theoretical models that have been proposed to explain the thermodiffusion of charged particles predict that S_T should scale with the square of the electric field near the particle surface; thus, most theoretical models would predict $S_T \propto Z^2$ if the screening length in the solvent is constant. However, many of the models also predict a dependence of S_T on the Debye screening length κ^{-1} and, unfortunately, we were not able to control the ionic strength of the lysozyme suspensions. (We could have, in principle, added salt to the suspensions of low ionic strength, but this would have introduced additional experimental uncertainties due to the electric fields generated by electrolytes in a temperature gradient.¹²) Different theoretical models give different predictions of the scaling of S_T with κ^{-1} . For example, the model of Fayolle et al.³⁶ predicts $S_T \propto \kappa$ for small particles ($\kappa R_h \ll 1$) and $S_T \propto \kappa^{-1}$ for large particles ($\kappa R_h \gg 1$); and, as we show below, the model of Derjaguin and Anderson³ suggests that S_T is independent of κ^{-1} for $\kappa R_h \ll 1$.

In Figure 5, we plot S_T as a function of ζ at $T \approx 35$ °C to emphasize the fact that S_T for these small proteins is not influenced by changes in ζ . We do note that, by coincidence, the screening length for each of these protein suspension varies in the opposite direction as the particle charge: $\kappa^{-1} \approx 4.8$, 7.9, 9.6, and 11.8 nm for the +9, +7, +5, and +3 proteins, respectively.

4. Discussion

Dependence of Thermodiffusion on Particle Size. Thermodiffusion of particles in liquids lacks an accepted theoretical description,^{9,11} and even a basic understanding of scaling with particle size is not established. In most cases, theories predict S_T to scale linearly with particle size.^{3,37–40} The review by Anderson³ describes how this scaling results from general considerations of the effective slip velocity created by a diffuse interfacial layer subjected to a gradient in temperature, electrostatic potential, or concentration. The model proposed by Andreev,⁶

(35) Zhang, X.; Wozniak, J. A.; Matthews, B. W. *J. Mol. Biol.* **1995**, *250*, 527–552.

(36) Fayolle, S.; Bickel, T.; Boiteux, S. L.; Würger, A. *Phys. Rev. Lett.* **2005**, *95*, 208301.

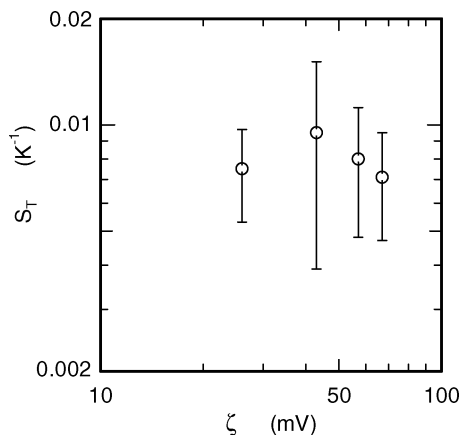


Figure 5. Soret coefficients as a function of ζ -potential for the protein suspensions of WT T4L and mutant variants of T4L at $T \approx 35$ °C.

on the other hand, predicts S_T to scale as $R_h^{3/2}$. Unfortunately, systematic thermodiffusion studies as a function of R_h are limited. Two noted exceptions are the recent experimental studies at room temperature by Duhr et al.⁹ and Vigolo et al.⁴¹ However, these studies do not support the same particle size dependence. Duhr et al. show that S_T scales as R_h^2 for carboxyl-modified PS spheres of varying sizes ($20 \text{ nm} \leq R_h \leq 2000 \text{ nm}$), where Vigolo et al. show that S_T scales much more like R_h , not R_h^2 , for microemulsion droplets of varying sizes ($1 \text{ nm} \leq R_h \leq 50 \text{ nm}$).

Our experiments also examine a relatively wide range of particle sizes; however, as shown in Figure 3, it is difficult to clearly distinguish between the effects of changing particle size and the effects of changing temperature. At high temperatures, where the Soret coefficients are positive, S_T appears to plateau and approach a constant value. This behavior suggests that S_T possesses a high-temperature limit; therefore, we have examined the particle size dependence of S_T at high temperatures in an attempt to deduce the scaling of S_T with particle radius. For this analysis, we follow the procedure used by Iacopini et al. and fit our S_T data to an empirical fitting function

$$S_T(T) = S_T^{\text{HT}} \left[1 - \exp\left(\frac{T^* - T}{T_o}\right) \right] \quad (3)$$

where S_T^{HT} represents the high- T limit, T^* is the temperature where S_T changes sign, and T_o represents the strength of the temperature effects.^{14,15} Figure 6 shows three examples of this fitting procedure. To emphasize the size dependence we observe at high temperatures, our asymptotic values of S_T in this high- T limit, S_T^{HT} , are provided in Figure 7 for WT T4L and the PS nanoparticles.

As shown in Figure 7, our results do not support a scaling of S_T with the square of the particle radius as was found by Duhr et al.;⁹ however, their data were measured near room temperature, not elevated temperatures, and their particle sizes were significantly larger, extending to $R_h \approx 2 \mu\text{m}$. Instead, we find that the scaling of S_T with particle size is consistent with a linear dependence on R_h .³ The size dependence we observe in the high- T limit is, however, strongly influenced by S_T^{HT} for the small

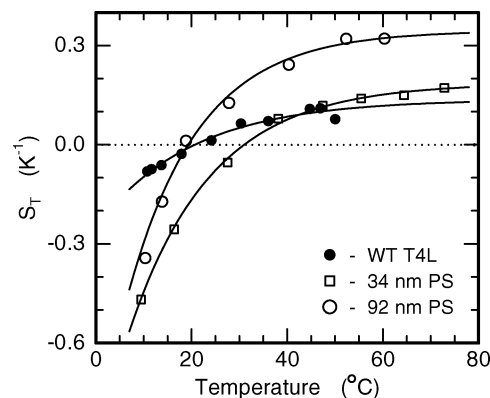


Figure 6. S_T data (symbols) for WT lysozyme, 34 nm PS, and 92 nm PS with comparisons to our fits using eq 3 (lines). The WT lysozyme data (filled circles) are multiplied by a factor of 10 to facilitate the comparisons. The fitting parameters for each respective data set are as follows: $S_T^{\text{HT}} = 0.0137 \pm 0.0019 \text{ K}^{-1}$, $T^* = 20.7$ °C, $T_o = 21 \pm 2$ °C for WT lysozyme; $S_T^{\text{HT}} = 0.186 \pm 0.02 \text{ K}^{-1}$, $T^* = 31$ °C, $T_o = 17.2 \pm 0.5$ °C for 32 nm PS; and $S_T^{\text{HT}} = 0.345 \pm 0.012 \text{ K}^{-1}$, $T^* = 19.3$ °C, $T_o = 14.5 \pm 1$ °C for 92 nm PS.

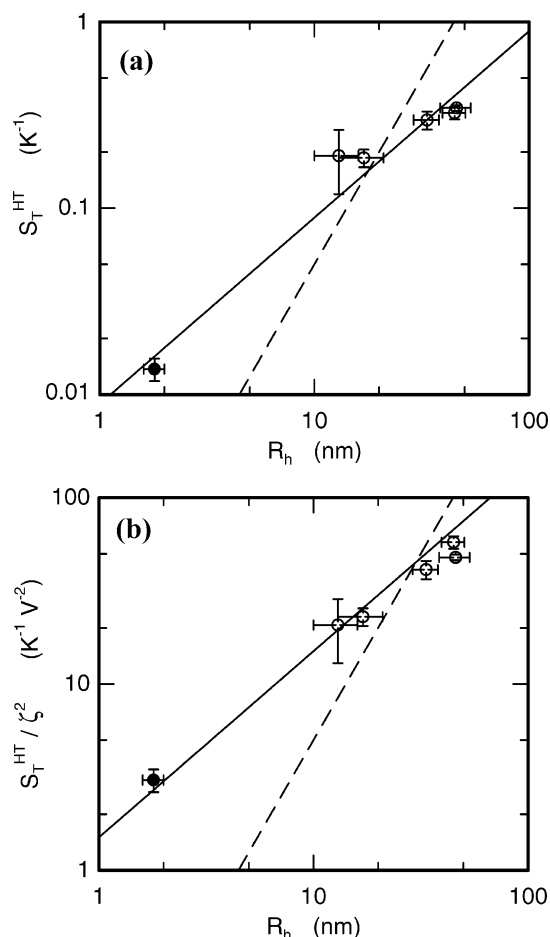


Figure 7. Size dependence of the thermodiffusion of carboxyl-functionalized PS spheres (open circles) and WT T4 lysozyme (filled circles) in the high-temperature limit. The solid lines are for $S_T \propto R_h$, and dashed lines are for $S_T \propto R_h^2$. (a) Soret coefficients measured in the high-temperature limit as a function of particle radius. (b) Soret data in (a) divided by ζ^2 .

(37) Bielenberg, J. R.; Brenner, H. *Physica A* **2005**, *356*, 279.

(38) Parola, A.; Piazza, R. *Eur. Phys. J. E* **2004**, *15*, 255.

(39) Schimpf, M. E.; Semenov, S. N. *J. Phys. Chem. B* **2001**, *105*, 2285.

(40) Morozov, K. I. In *On the theory of the Soret effect in colloids*; Köhler, W., Wiegand, S., Eds.; Springer-Verlag: Heidelberg, 2002; Vol. 584, Chapter 3, pp 38–60.

(41) Vigolo, D.; Brambilla, G.; Piazza, R. *Phys. Rev. E* **2007**, *75*, 040401.

lysozyme; and the conclusions that we can draw from the data shown in Figure 7 are also complicated by differences in surface chemistry between lysozyme and PS. The surface chemistry of a particle has, at least in some cases, been shown to influence

thermodiffusion.⁴² We believe, however, that the factor of 50 difference in particle radius and S_T shown in Figure 7 spans a great enough range to support our conclusion that S_T scales linearly with R_h , not as R_h^2 .

Possible Dependence on the Thermal Expansivity of Water.

Recently, the thermal expansion of the solvent has been proposed as an important factor in determining the temperature dependence of S_T .^{2,15} If the particle and solvent do not interact chemically

$$S_T \propto \frac{D_s}{D_c} \alpha \quad (4)$$

where D_s is the solvent's self-diffusivity, α is the solvent's thermal expansivity, and D_c is the concentration diffusion coefficient of the particle.² In general, D_s and D_c will have approximately the same temperature dependence; therefore, S_T/α is predicted to be independent of temperature. In ref 15, the connection between the T dependence of S_T and the thermal expansivity of water has been experimentally investigated for a wide variety of different macromolecular and colloidal suspensions (e.g., DNA, proteins, micelles, and PS nanoparticles). We analyzed our data following the procedures of ref 15: while the temperature dependence of S_T measured relative to its value at 4 °C bears some resemblance to the expansivity of water, we do not believe that our data are in good agreement with the prediction of eq 4.

Electrostatic Contributions to Thermodiffusion. In an attempt to identify the fundamental mechanisms responsible for the temperature-dependent thermodiffusion of charged particles in water, we have examined the predictions of several theories. We give special attention in this section to the four different single-particle models proposed by Anderson,³ Bringuier et al.,⁴³ Duhr et al.,⁹ and Morozov⁵ that are based on the electrostatics of the double layer and scale with the square of the particle surface potential. In the following, we first review each model; then, a quantitative numerical comparison with our S_T data is provided. We note that the ζ -potentials of our studied particles are greater than $k_B T$; therefore, the connection between our S_T data and the predictions of the following models are highly dependent on whether or not these models are still relatively accurate for $|\zeta| > 25$ mV.

Model by Anderson. We first describe the theory originally derived by Derjaguin¹⁶ and later adapted by Anderson.³ The original work of Derjaguin considered thermoosmosis of an electrolyte in a porous medium. Anderson then reformulated this description to describe the thermophoresis of particles in liquids. In this theory, when the particles are large relative to the thickness of the interfacial layer ($\kappa R_h \gg 1$), Anderson predicts the thermodiffusion coefficient to be

$$D_T = -\frac{2}{\eta T} \left[\frac{2\Lambda_l}{2\Lambda_l + \Lambda_p} \right] \int_0^\infty y h(y) dy \quad (5)$$

where $h(y)$ is the enthalpy density at a distance y from the particle surface, and Λ_p and Λ_l are the thermal conductivities of the particle and the liquid, respectively.¹² The integral term in eq 5 is the first moment of the local specific enthalpy increment, $h(y)$, from the solid/liquid interface. The change in the enthalpy density, $h(y)$, due to the polarization of water molecules in the double layer has been evaluated previously in the low-potential limit:⁴⁴ $h_E(y) = 1/2(\epsilon + T\partial\epsilon/\partial T)E^2(y)$, where ϵ is the static dielectric constant of water, $E(y)$ is the electric field, and $1/2(\epsilon E^2)$ is the

free-energy density. We approximate the electric field as $E(y) = \kappa\zeta \exp(-\kappa y)$, where ζ is the ζ -potential and κ^{-1} is the Debye screening length. This is a good approximation for $E(y)$ in a flat double layer⁴⁵ when $\zeta \lesssim 2k_B T/e$. In this case, the electrostatic contribution to S_T due to the polarization of water molecules in the double-layer is

$$S_T^{\text{Anderson}} = -\frac{3\pi R_h}{2k_B T^2} \left[\frac{2\Lambda_l}{2\Lambda_l + \Lambda_p} \right] \left(\epsilon + T \frac{\partial\epsilon}{\partial T} \right) \zeta^2 \quad (6)$$

given $\kappa R_h \gg 1$ and $\zeta \lesssim 2k_B T/e$.

Equation 6 is derived for a large particle ($\kappa R_h \gg 1$). Derjaguin's original work also discusses the thermoosmosis of the electrolyte in the narrow pores relative to the double-layer thickness¹⁶ ($\kappa R_h \ll 1$). In this case, $\kappa R_h \ll 1$, the integral term in eq 5 simply requires multiplication by 2/3. To evaluate the integral term in eq 5, we still calculate the enthalpy density based on the polarization of the water molecules in the double layer as before. However, we no longer use the electric field for a flat double layer, but instead use the electric field for a spherical particle $E(y) = \zeta R_h [1 + \kappa(R_h + y)] \exp(-\kappa y) / (R_h + y)^2$. In this case, we estimate the electrostatic contribution to S_T due to the polarization of water molecules in the double layer as simply eq 6 multiplied by 4/3; i.e.

$$S_T^{\text{Anderson}} = -\frac{2\pi R_h}{k_B T^2} \left[\frac{2\Lambda_l}{2\Lambda_l + \Lambda_p} \right] \left(\epsilon + T \frac{\partial\epsilon}{\partial T} \right) \zeta^2 \quad (7)$$

given $\kappa R_h \ll 1$ and $\zeta \lesssim 2k_B T/e$. Because the particles studied in this work, along with the particles in many other charged-stabilized dispersions, have ζ -potentials much greater than $k_B T$, we have compared the predictions of the analytical solutions above (eqs 6 and 7) with the numerical solutions of S_T based on the exact expression for the electric fields in the double layer derived from Poisson–Boltzmann theory.⁴⁵ As expected, we find excellent agreement for $|\zeta| \lesssim 50$ mV. The agreement is also surprisingly good for highly charged particles. For example, we find for $|\zeta| \approx 100$ mV that eqs 6 and 7 are within $\sim 10\%$ of the numerical results when $\kappa^{-1} \gtrsim 5$ nm and deviate from the numerical solutions by, at most, $\sim 30\%$ when $\kappa^{-1} \approx 0.5$ nm.

Model by Bringuier and Bourdon. In the model proposed by Bringuier et al.,⁴³ the Soret coefficient is defined as $S_T = 1/T + (1/k_B T) \partial W^{\text{dl}} / \partial T$, where W^{dl} is the electrical work required to form the double layer. The first term in this expression, $S_T = 1/T$, is the kinetic contribution due to Brownian motion of the particle. As discussed in ref 45, W^{dl} must be positive and within the limits $1/2(Q\Psi) < W^{\text{dl}} < Q\Psi$, where Q is the total surface charge, Ψ is the surface potential, and in the low-potential limit $W^{\text{dl}} \approx 1/2(Q\Psi)$. We consider the case for a moderately charged spherical particle and approximate $Q = 4\pi\epsilon R_h(1 + \kappa R_h)\zeta$ and $\Psi = \zeta$. In this case, we predict the contribution to S_T due to the formation of the double layer as

$$S_T^{\text{Bringuier}} = \frac{1}{T} + \frac{1}{k_B T} \frac{\partial W_{\text{min}}^{\text{dl}}}{\partial T} = \frac{1}{T} + \frac{W_{\text{min}}^{\text{dl}}}{k_B T^2} \times \left[\frac{T}{\epsilon} \frac{\partial\epsilon}{\partial T} + \frac{2T}{\zeta} \frac{\partial\zeta}{\partial T} - \frac{\kappa R_h \left(1 + \frac{T}{\epsilon} \frac{\partial\epsilon}{\partial T} \right)}{2(1 + \kappa R_h)} \right] \quad (8)$$

where $W_{\text{min}}^{\text{dl}} \equiv 2\pi\epsilon R_h(1 + \kappa R_h)\zeta^2$. Thus, for $\kappa R_h \gg 1$ and $\partial\zeta/\partial T \approx 0$, we expect the electrostatic contribution to be

(42) Jeon, S. J.; Schimpf, M. E.; Nyborg, A. *Anal. Chem.* **1997**, *69*, 3442.

(43) Bringuier, E.; Bourdon, A. *Phys. Rev. E* **2003**, *67*, 011404.

(44) Churaev, N. V.; Deryagin, B. V.; Zolotarev, P. P. *Dokl. Akad. Nauk. SSSR* **1968**, *183*, 1139.

(45) Verwey, E. J. W.; Overbeek, J. T. G. *Theory of the stability of lyophobic colloids*; Elsevier Publishing Co.: New York, 1948; pp 51–65.

$$S_T^{\text{Bringuier}} = -\frac{\pi\epsilon\kappa R_h^2}{k_B T^2} \left(1 - \frac{T}{\epsilon} \frac{\partial\epsilon}{\partial T}\right) \zeta^2 \quad (9)$$

We note that similar relations based on the free energy of the double layer have been utilized in recent publications by other authors.^{9,36,46,47}

Model by Duhr and Braun. The model proposed by Duhr et al.⁹ also describes thermodiffusion in terms of the free energy of the double layer. However, in this formalism, the Gibbs-free enthalpy G_H is used instead of W^{dl} ; i.e., the Soret coefficient is defined as $S_T = 1/T + (1/k_B T) \partial G_H / \partial T$. Duhr et al. predict G_H to have three contributions based on the differences in the entropy associated with Brownian motion, water hydration, and ionic screening; the Soret coefficient is then $S_T = S_T^{\text{BM}} + S_T^{\text{hyd}} + S_T^{\text{ionic}}$, where the first term, S_T^{BM} , is due to the Brownian motion of the particle, the second term, S_T^{hyd} , is due to the entropy of hydration of the water molecules, and the third term, S_T^{ionic} , is due to the ionic screening of the particle's charge.

To calculate S_T^{ionic} , Duhr et al. approximate the Gibbs-free enthalpy as $G_H^{\text{ionic}} = Q_{\text{eff}}^2 / (8\pi\epsilon\kappa R_h^2)$, where Q_{eff} is the effective surface charge of the particle. The effective charge of the particle is assumed to be independent of temperature. In this case, the Soret coefficient is $S_T^{\text{ionic}} = \beta Q_{\text{eff}}^2 / (16\pi\epsilon\kappa R_h^2 k_B T^2)$, where the temperature dependence of ϵ and κ give rise to the factor $\beta = 1 - (T/\epsilon)(\partial\epsilon/\partial T)$. To express S_T^{ionic} in terms of the ζ -potential, we approximate the effective surface charge of the particle as before $Q_{\text{eff}} = 4\pi\epsilon R_h (1 + \kappa R_h) \zeta$. The electrostatic contribution to S_T can then be expressed in the form

$$S_T^{\text{Duhr}} = \frac{\pi\epsilon(1 + \kappa R_h)^2}{\kappa k_B T^2} \left(1 - \frac{T}{\epsilon} \frac{\partial\epsilon}{\partial T}\right) \zeta^2 \quad (10)$$

For $\kappa R_h \gg 1$, this prediction reduces to

$$S_T^{\text{Duhr}} = \frac{\pi\epsilon\kappa R_h^2}{k_B T^2} \left(1 - \frac{T}{\epsilon} \frac{\partial\epsilon}{\partial T}\right) \zeta^2 \quad (11)$$

Equation 11 is the negative of eq 9. The sign difference between eq 9 and eq 11 is discussed in ref 47 and originates from considering the reversible work to charge the double layer as opposed to its free energy; see eqs 41 and 42 therein.

Model by Morozov. In the description by Morozov,⁵ particle velocities are derived from the basis that temperature gradients induce nonuniform electric stresses in the double layer; that is, thermodiffusion is due to unbalanced electrostatic potentials and electrolyte distributions on opposite sides of the particle. In the limit of an infinitely thin double layer, $\kappa^{-1} \rightarrow 0$, and small volume fractions of particles, Morozov's analytic solution for the Soret coefficient is

$$S_T^{\text{Morozov}} = \frac{R_h}{2L_B T} \left[\frac{3\Lambda_1}{2\Lambda_1 + \Lambda_p} \right] \times \left[\zeta_D^2 - \left(24 + 8 \frac{T}{\epsilon} \frac{\partial\epsilon}{\partial T}\right) \ln \cosh \frac{\zeta_D}{4} \right] \quad (12)$$

where $\zeta_D = e\zeta/k_B T$ is the dimensionless ζ -potential, and L_B is the Bjerrum length. (For $\kappa^{-1} > 0$, no analytic solution exists, and the problem can only be solved numerically; however, as shown by Morozov, if $|\zeta| \approx 4k_B T/e$, then the numerical solutions of S_T

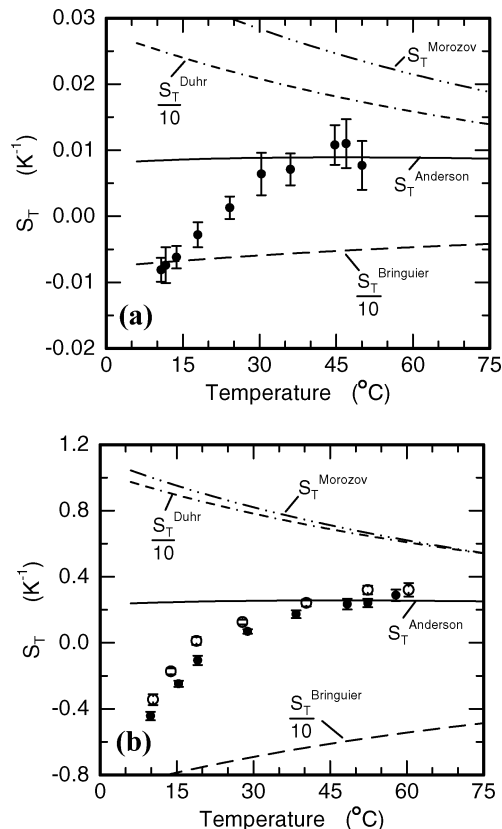


Figure 8. Soret coefficients (symbols) as a function of temperature with comparisons to the predictions of Anderson, Bringuier et al. (eq 8), Duhr et al. (eq 10), and Morozov (eq 12). The predictions by Bringuier et al. (eq 8) and Duhr et al. (eq 10) are divided by a factor of 10 to facilitate the comparisons. In the upper plot (a), eq 7 is used for Anderson's prediction; and in the bottom plot (b), eq 6 is used for Anderson's prediction. (a) Soret coefficients for WT T4 lysozyme. Temperature-independent model parameters: $\zeta \approx 75$ mV, $R_h \approx 1.8$ nm, $I \approx 4.0$ mM. (b) Soret coefficients for 90 nm PS (filled circles) and 92 nm PS (open circles). Temperature-independent model parameters: $\zeta \approx -80$ mV, $R_h \approx 45.5$ nm, $I \approx 1.0$ mM.

for $\kappa^{-1} > 0$ do not differ significantly from the analytical solution of S_T provided above (eq 12); see Figure 1 in ref 5. Therefore, in Morozov's description of thermodiffusion, as long as $|\zeta| \approx 4k_B T/e$, then eq 12 is also a good approximation for S_T even if $\kappa^{-1} > 0$.)

Comparison with Theories. Figure 8 shows the predictions of Anderson, Bringuier et al., Duhr et al., and Morozov with comparisons to our S_T data for (a) WT T4L and (b) 90 and 92 nm PS nanoparticles. In this analysis, the small contributions due to thermal expansion ($\partial R_h / \partial T$) are ignored, and constant ζ -potentials for these nanoparticles at room temperature are used. The temperature dependence of all other model parameters—i.e., ϵ , κ , L_B , Λ_1 , and Λ_p —are calculated or taken from literature.⁴⁸

We did not take into account the temperature dependence of the ζ -potential, because (i) we are unaware how the formal charge of lysozyme varies with temperature, and (ii) the temperature dependence of the surface charge σ for the carboxyl-functionalized PS spheres at ~ 6.5 pH is small in comparison to the temperature dependence of the dielectric constant of water; i.e., $|\partial \ln \sigma / \partial \ln T| < |\partial \ln \epsilon / \partial \ln T|$. This comparison is based on a calculation of $\partial \ln \sigma / \partial \ln T$ using eqs 2–4 in ref 49 and literature values for

(48) The dielectric constant and thermal conductivity of water were taken from refs 54 and 32, respectively. A thermal conductivity of $\Lambda_{\text{PS}} \approx 1.51 + 0.003(T - 293.15) \times 10^{-3} \text{ W cm}^{-1} \text{ K}^{-1}$ was used for polystyrene based on the data in refs 55, 56, and 57. The thermal conductivity for lysozyme was approximated as that of PS.

(46) Piazza, R.; Guarino, A. *Phys. Rev. Lett.* **2002**, *88*, 208302.

(47) Dhont, J. K. G.; Wiegand, S.; Duhr, S.; Braun, D. *Langmuir* **2007**, *23*, 1674.

the temperature dependence of the ionization constants of carboxylic acids.⁵⁰ The T -dependence for the pK_a of acetic acid is, like other carboxylic acids, parabolic with a minimum at ~ 25 °C; e.g., $pK_a(T) \approx 4.76 + 0.00004(298 - T)^2$. Therefore, we expect the apparent pK_a of our carboxyl-functionalized particles to increase by, at most, 0.1 unit between 25 and 75 °C. In this case, we calculate, for instance, $\partial \ln \sigma / \partial \ln T \approx -0.1$ for the 92 nm carboxyl spheres at $T \gtrsim 30$ °C, where the T -dependence of the dielectric constant of water is $\partial \ln \epsilon / \partial \ln T \approx -1.4$.

As shown in Figure 8, our measured Soret coefficients are consistent with the description of Anderson but only at high temperatures. However, none of the electrostatic models discussed here can explain the observed temperature dependence of S_T . With the exception of the model by Bringuier *et al.*, Soret coefficients based on purely electrostatic interactions always predict $S_T > 0$.

5. Conclusions

Our experiments show that the temperature dependence of the thermodiffusion of 2 nm diameter, positively charged proteins and 100 nm diameter, negatively charged polystyrene nanoparticles are remarkable similar: S_T is negative at low temperature and positive at high temperatures greater than ~ 25 °C. This same qualitative temperature dependence has recently been observed by others in studies with PS,¹⁵ lysozyme,^{14,15} and other charged macromolecular particles in aqueous solutions.¹⁵ Therefore, these results suggest to us that thermodiffusion of charged

particles in aqueous solutions is highly dependent on the properties of the solvent, e.g., the response of water molecules to the high electric fields of the double layer.

At high temperatures, $T \gtrsim 50$ °C, S_T approaches a constant value that scales linearly with the particle radius. Moreover, in this high-temperature limit, S_T is consistent with the predictions of an electrostatic model proposed by Derjaguin and Anderson that is based on the enthalpy changes due to polarization of water molecules by the electric fields in the double layer. We find that S_T can be accurately predicted in the high-temperature limit for charged particles with ζ -potentials greater in magnitude than ~ 60 mV. For small particles with $|\zeta| \lesssim 50$ mV, the model predicts a stronger dependence on ζ -potential than we observe. Furthermore, the electrostatic model cannot describe the strong temperature dependence of S_T for the wide variety of aqueous suspensions we have studied. At lower temperatures, other mechanisms may play an increasingly important role in driving thermodiffusion. In this regard, we note the recent description by Duhr *et al.*⁹ that includes nonelectrostatic contributions to S_T based on changes in water structure or changes in hydration entropies at the particle/water interface.

These conclusions are based on a quantitative numerical comparison between our experimental results and existing single-particle theories of electrostatic origin. With exception of the model by Morozov,⁵ all electrostatic models discussed are derived for $|\zeta| \leq 25$ mV; therefore, this numerical comparison is highly dependent on the assumption that these models are still reasonably accurate for $|\zeta| > 25$ mV. In addition, we cannot exclude the possibility that particle–particle interactions have a significant influence on our experimental results.

Acknowledgment. This work is based upon work supported by the STC Program of the National Science Foundation under Agreement Number CTS-0120978. The authors are grateful to Dr. Lori K. Sanders, Wujing Xian, and Dr. Brian W. Matthews for their contributions in preparation of the protein suspensions.

LA700489E

(49) Behrens, S. H.; Christl, D. I.; Emmerzael, R.; Schurtenberger, P.; Borkovec, M. *Langmuir* **1998**, *16*, 2566.

(50) Serjeant, E. P.; Dempsey, B. In *Ionisation constants of organic acids in aqueous solution*; Pergamon Press: Oxford, 1979; Vol. 23, pp 19–21.

(51) Braibanti, A.; Fiscaro, E.; Ghiozzi, A.; Compari, C. *Thermochim. Acta* **1996**, *286*, 51.

(52) *Thermophysical Properties of Matter*; Touloukian, Y. S., Ho, C. Y., Eds.; Plenum: New York, 1970; Vol. 5.

(53) Cahill, D. G. *Rev. Sci. Instrum.* **1990**, *61*, 802.

(54) Meissner, T.; Wentz, F. J. *IEEE Transactions on Geoscience and Remote Sensing* **2004**, *42*, 1836–1849.

(55) Kikuchi, T.; Takahashi, T.; Koyama, K. *J. Macromol. Sci.* **2003**, *B42*, 1097.

(56) Dashora, P.; Gupta, G. *Polymer* **1996**, *37*, 231.

(57) Sombatsompop, N.; Wood, A. K. *Polym. Test.* **1997**, *16*, 203.